NIH Public Access
Author Manuscript
Cell. Author manuscript; available in PMC 2014 May 09.

Published in final edited form as:
Cell. 2013 May 9; 153(4): 840–854. doi:10.1016/j.cell.2013.04.023.

The mTORC1 pathway stimulates glutamine metabolism and cell proliferation by repressing SIRT4

Alfred Csibi[1], **Sarah-Maria Fendt**[2,$], **Chenggang Li**[3,$], **George Poulogiannis**[4,$], **Andrew Y. Choo**[1], **Douglas J. Chapski**[1], **Seung Min Jeong**[1], **Jamie Dempsey**[1], **Andrey Parkhitko**[3], **Tasha Morrison**[3], **Elizabeth Henske**[3], **Marcia Haigis**[1], **Lewis C. Cantley**[4], **Gregory Stephanopoulos**[2], **Jane Yu**[3], and **John Blenis**[1,§]

[1]Department of Cell Biology, Harvard Medical School, Cambridge, Massachusetts 02139, USA

[2]Department of Chemical Engineering, Massachusetts Institute of Technology, Cambridge, Massachusetts 02139, USA

[3]Division of Pulmonary and Critical Care Medicine, Department of Medicine, Brigham and Women's Hospital, Harvard Medical School, Boston, MA 02115, USA.

[4]Division of Signal Transduction, Beth Israel Medical Center and Department of Systems Biology, Harvard Medical School, Boston, MA 02115, USA.

Summary

Proliferating mammalian cells use glutamine as a source of nitrogen and as a key anaplerotic source to provide metabolites to the tricarboxylic acid cycle (TCA) for biosynthesis. Recently, mTORC1 activation has been correlated with increased nutrient uptake and metabolism, but no molecular connection to glutaminolysis has been reported. Here, we show that mTORC1 promotes glutamine anaplerosis by activating glutamate dehydrogenase (GDH). This regulation requires transcriptional repression of *SIRT4*, the mitochondrial-localized sirtuin that inhibits GDH. Mechanistically, mTORC1 represses *SIRT4* by promoting the proteasome-mediated destabilization of cAMP response element binding-2 (CREB2). Thus, a relationship between mTORC1, SIRT4 and cancer is suggested by our findings. Indeed, *SIRT4* expression is reduced in human cancer, and its overexpression reduces cell proliferation, transformation and tumor development. Finally, our data indicate that targeting nutrient metabolism in energy-addicted cancers with high mTORC1 signaling may be an effective therapeutic approach.

Introduction

Nutrient availability plays a pivotal role in the decision of a cell to commit to cell proliferation. In conditions of sufficient nutrient sources and growth factors (GFs), the cell generates enough energy and acquires or synthesizes essential building blocks at a sufficient rate to meet the demands of proliferation. Conversely, when nutrients are scarce, the cell responds by halting the biosynthetic machinery and by stimulating catabolic processes such

© 2013 Elsevier Inc. All rights reserved.

§Correspondence: john_blenis@hms.harvard.edu.
$Current Address: Flemish Institute of Biotechnology (VIB), Vesalius Research Center, Leuven, Belgium

Publisher's Disclaimer: This is a PDF file of an unedited manuscript that has been accepted for publication. As a service to our customers we are providing this early version of the manuscript. The manuscript will undergo copyediting, typesetting, and review of the resulting proof before it is published in its final citable form. Please note that during the production process errors may be discovered which could affect the content, and all legal disclaimers that apply to the journal pertain.

*These authors contributed equally to this work.

NIH-PA Author Manuscript
NIH-PA Author Manuscript
NIH-PA Author Manuscript

NIH-PA Author Manuscript

NIH-PA Author Manuscript

NIH-PA Author Manuscript

as fatty acid oxidation and autophagy to provide energy maintenance (Vander Heiden et al., 2009). Essential to the decision process between anabolism and catabolism is the highly conserved, atypical Serine/Threonine kinase mammalian Target of Rapamycin Complex 1 (mTORC1), whose activity is deregulated in many cancers (Menon and Manning, 2008). This complex, which consists of mTOR, Raptor, and mLST8, is activated by amino acids (aa), GFs (insulin/IGF-1) and cellular energy to drive nutrient uptake and subsequently proliferation (Yecies and Manning, 2011). The molecular details of these nutrient-sensing processes are not yet fully elucidated, but it has been shown that aa activate the Rag GTPases to regulate mTORC1 localization to the lysosomes (Kim et al., 2008; Sancak et al., 2008); and GFs signal through the PI3K-Akt or the extracellular signal-regulated kinase (ERK)-ribosomal protein S6 kinase (RSK) pathways to activate mTORC1 by releasing the Ras homolog enriched in brain (RHEB) GTPase from repression by the tumor suppressors, tuberous sclerosis 1 (TSC1)– TSC2 (Inoki et al., 2002; Manning et al., 2002; Roux et al., 2004). Finally, low energy conditions inhibit mTORC1 by activating AMPK and by repressing the assembly of the TTT-RUVBL1/2 complex. (Inoki et al., 2003; Gwinn et al., 2008; Kim et al., 2013).

Glutamine, the most abundant amino acid in the body plays an important role in cellular proliferation. It is catabolized to α-ketoglutarate (αKG), an intermediate of the tricarboxylic acid (TCA) cycle through two deamination reactions in a process termed glutamine anaplerosis (DeBerardinis et al., 2007). The first reaction requires glutaminase (GLS) to generate glutamate, and the second occurs by the action of either glutamate dehydrogenase (GDH) or transaminases. Incorporation of αKG into the TCA cycle is the major anaplerotic step critical for the production of biomass building blocks including nucleotides, lipids and aa (Wise and Thompson, 2010). Recent studies have demonstrated that glutamine is also an important signaling molecule. Accordingly, it positively regulates the mTORC1 pathway by facilitating the uptake of leucine (Nicklin et al., 2009) and by promoting mTORC1 assembly and lysosomal localization (Duran et al., 2012; Kim et al., 2013).

Commonly occurring oncogenic signals directly stimulate nutrient metabolism, resulting in nutrient addiction. Oncogenic levels of Myc have been linked to increased glutamine uptake and metabolism through a coordinated transcriptional program (Wise et al., 2008; Gao et al., 2009). Hence, it is not surprising that cancer cells are addicted to glutamine (Wise and Thompson, 2010). Thus, considering the prevalence of mTORC1 activation in cancer and the requirement of nutrients for cell proliferation, understanding how mTORC1 activation regulates nutrient levels and metabolism is critical. Activation of the mTORC1 pathway promotes the utilization of glucose, another nutrient absolutely required for cell growth. However, no study has yet investigated if and how the mTORC1 pathway regulates glutamine uptake and metabolism. Here, we discover a novel role of the mTORC1 pathway in the stimulation of glutamine anaplerosis by promoting the activity of GDH. Mechanistically, mTORC1 represses the transcription of *SIRT4*, an inhibitor of GDH. SIRT4 is a mitochondrial-localized member of the sirtuin family of NAD-dependent enzymes known to play key roles in metabolism, stress response and longevity (Haigis and Guarente, 2006). We demonstrate that the mTORC1 pathway negatively controls *SIRT4* by promoting the proteasome-mediated degradation of cAMP-responsive element-binding (CREB) 2. We reveal that SIRT4 levels are decreased in a variety of cancers, and when expressed, SIRT4 delays tumor development in a *Tsc2*−/− mouse embryonic fibroblasts (MEFs) xenograft model. Thus, our findings provide new insights into how mTORC1 regulates glutamine anaplerosis, contributing therefore to the metabolic reprogramming of cancer cells, an essential hallmark to support their excessive needs for proliferation.

NIH-PA Author Manuscript

NIH-PA Author Manuscript

NIH-PA Author Manuscript

Results

The mTORC1 pathway regulates glutamine metabolism via GDH

The activation of the mTORC1 pathway has recently been linked to glutamine addiction of cancer cells (Choo et al., 2010), yet it remains to be resolved if mTORC1 serves as a regulator of glutamine anaplerosis. To investigate this possibility, we first determined the effect of mTORC1 activity on glutamine uptake. We measured glutamine uptake rates in *Tsc2* wild-type (WT) and *Tsc2*−/− MEFs. We found that *Tsc2*−/− MEFs consumed significantly more glutamine (Figure 1A), showing that mTORC1 activation stimulates the uptake of this nutrient. In addition, re-expression of Tsc2 in *Tsc2*−/− cells reduced glutamine uptake (Figure S1A). Similarly, mTORC1 inhibition with rapamycin resulted in decreased glutamine uptake in MEFs (Figure 1A). The decreased on glutamine uptake was significantly reduced after 6h of rapamycin treatment when compared to control (data not shown). To further confirm the role of mTORC1 on glutamine uptake, we used human embryonic kidney (HEK) 293T cells stably expressing either WT-RHEB or a constitutively active mutant (S16H) of RHEB. Increased mTORC1 signaling, as evidenced by sustained phosphorylation of S6K1 and its target rpS6, was observed in RHEB-expressing cells (Figure S1B). The activation of the mTORC1 pathway nicely correlated with an increase in glutamine consumption, therefore confirming that changes in mTORC1 signaling are reflected in cellular glutamine uptake (Figure S1B). To determine whether the modulation of glutamine uptake by the mTORC1 pathway occurs in cancer cells, we examined glutamine uptake rates in conditions of mTORC1 inhibition in human epithelial tumor cell lines, including the colon carcinoma DLD1, and the prostate cancer DU145. Rapamycin treatment resulted in decreased proliferation (data not shown) and yielded a decreased glutamine uptake in both cell lines (Figure 1B & data not shown). Glutamine is the major nitrogen donor for the majority of ammonia production in cells (Figure 1C) (Shanware et al., 2011). Consistent with decreased glutamine uptake, we found that ammonia levels were also diminished after rapamycin treatment (Figure S1C).

We next examined the fate of glutamine in conditions of mTORC1 inhibition, using gas chromatography/mass spectrometry (GC/MS) analysis to monitor the incorporation of uniformly labeled [U-$^{13}C_5$]-Glutamine into TCA cycle intermediates. Direct glutamine contribution to ĮKG (m+5), succinate (m+4), malate (m+4) and citrate (m+4) was decreased in rapamycin treated cells (Figure S1D) indicating that rapamycin impaired glutamine oxidation and subsequent carbon contribution into the TCA cycle.

To test whether glutamine uptake or glutamine conversion is limiting, we measured the intracellular levels of glutamine and glutamate in DLD1 cells. Increased levels of glutamine and/or glutamate will show that the catalyzing enzyme activity is limiting and not glutamine transport itself (Fendt et al., 2010). Rapamycin treatment resulted in increased intracellular levels of both glutamine and glutamate, showing that glutamate to αKG conversion is the critical limiting reaction (Figures 1D & 1E). To further confirm the implication of the glutamate catalyzing reaction we also measured αKG levels. If glutamate conversion is indeed critical we expect no alteration in αKG levels. This is expected because αKG is downstream of the potentially limiting glutamate conversion step, and it has been shown that product metabolite concentrations of limiting metabolic enzymes stay unaltered, while the substrate metabolite concentrations change to keep metabolic homeostasis (Fendt et al., 2010). We found that αKG levels were unaltered after rapamycin treatment, corroborating that the limiting enzymatic step is glutamate conversion (Figure 1F). To further confirm the limitation in glutamate-to-αKG conversion, we measured flux through this reaction. Strikingly, this flux was significantly reduced during rapamycin treatment (Figure 1G). Additionally, the inhibition of mTORC1 resulted in increased glutamate secretion (Figure

NIH-PA Author Manuscript

NIH-PA Author Manuscript

NIH-PA Author Manuscript

1H), thus confirming that the glutamate-to-αKG conversion step is a major bottleneck in the glutamine pathway during rapamycin treatment.

Glutamate conversion can be conducted by GDH (Figure 1C), suggesting that the mTORC1 pathway potentially regulates this enzyme. In agreement, rapamycin treatment resulted in decreased GDH activity in DLD1 cells (Figure 1I). To exclude that transaminases play a role in the mTORC1-induced regulation of glutamine metabolism, we used amin ooxyacetate (AOA) at a concentration shown to effectively inhibit the two predominant transaminases, alanine aminotransferase (ALT) and aspartate aminotransferase (AST) (Figure 1C) (Wise et al., 2008), or rapamycin in the presence of α-^{15}N-labeled glutamine. Subsequently, we measured ^{15}N-labeling patterns and metabolite levels of alanine, an amino acid that is predominately produced by a transaminase-catalyzed reaction (Possemato et al., 2011). We found that AOA dramatically decreased ^{15}N contribution and metabolite levels of alanine, while rapamycin only mildly affected the ^{15}N contribution to this amino acid and showed no effect on alanine levels compared to the control condition (Figures 1J & S1E). In conclusion, these data demonstrate that GDH, not transaminases, plays a major role in the regulation of glutamine metabolism downstream of mTORC1.

mTORC1 controls GDH activity by repressing SIRT4

As our results show that mTORC1 regulates glutamate dehydrogenase, we sought to identify the molecular mechanism. SIRT4 is a negative regulator of GDH activity through ADP-ribosylation (Haigis et al., 2006), thus suggesting that mTORC1 potentially controls this step of glutamine metabolism via SIRT4. To test this possibility, we first assessed the ADP-ribosylation status of GDH by introducing biotin-labeled NAD followed by immunoprecipitation using avidin-coated beads. Rapamycin treatment led to an increase in the mono-ADP-ribosylation status of GDH, similar to that observed in cells stably expressing SIRT4 (Figure 2A). Importantly, we found that the knockdown of SIRT4 abrogated the rapamycin-induced decrease in the activity of GDH (Figures 2B & S2A). Strikingly, SIRT4 protein levels were increased upon mTORC1 inhibition in MEFs (Figures 2C). This regulation was confirmed in both DLD1 and DU145 cells (Figures 2D). Remarkably, rapamycin potently increased SIRT4 levels after 6h of treatment (Figure S2B), correlating with reduced glutamine consumption at the same time point (data not shown). In contrast, SIRT4 levels were not influenced by the treatment of MEFs with U0216, an inhibitor of MEK1/2 in the MAPK pathway (Figure S2C). All other mTOR catalytic inhibitors tested in *Tsc2*−/− MEFs also resulted in increased SIRT4 protein levels (Figure S2D). To evaluate a potential regulation of SIRT4 by mTORC2, we performed RNA interference (RNAi) experiments of either raptor or the mTORC2 component, rictor, in *Tsc2*−/− MEFs. The knockdown of raptor, but not rictor, was sufficient to increase SIRT4 protein levels, confirming the role of the mTORC1 pathway in the regulation of SIRT4 (Figure 2E). To investigate whether mTORC1 regulation of SIRT4 occurs in tumor samples, a TSC-xenograft model was used. We injected a *TSC2*−/− rat leiomyoma cell line; ELT3 cells, expressing either an empty vector (V3) or TSC2 (T3), in the flank of nude mice. SIRT4 levels were dramatically increased in TSC2-expressing tumors compared to empty vector samples (Figure S2E). In addition, we assessed the levels of SIRT4 in both ELT3 xenograft tumors and in mouse *Tsc2*+/− liver tumors after rapamycin treatment. As expected, these tumor samples exhibited robust elevation of SIRT4 after rapamycin treatment (Figures 2F & S2F). Thus, these data demonstrate that the mTORC1 pathway represses SIRT4 in several tumor systems.

CREB2 regulates the transcription of SIRT4 in an mTORC1-dependent fashion

We next asked whether the mTORC1-dependent regulation of SIRT4 occurred at the mRNA level. Quantitative RT-PCR results show that rapamycin treatment significantly increased

NIH-PA Author Manuscript

NIH-PA Author Manuscript

NIH-PA Author Manuscript

the expression of *SIRT4* mRNA in *Tsc2*−/− MEFs (Figure 3A). *SIRT4* mRNA levels were dramatically reduced in *Tsc2*−/− MEFs compared to their WT counterpart (Figure 3B). Similar results were obtained from transcriptional profiling analysis of the *SIRT4* gene from a previously published dataset (GSE21755) (Figure 3C) (Duvel et al. 2010). Altogether, our data demonstrate that mTORC1 negatively regulates the transcription of *SIRT4*. To identify candidate transcription factors regulating *SIRT4*, we analyzed the nucleotide sequence of the human *SIRT4* promoter region. We used the TFSEARCH program, a computer algorithm available at http://mbs.cbrc.jp/research/db/TFSEARCH.html, and identified 21 potential transcription factors that may bind directly to and modulate the *SIRT4* promoter activity (see Table 1 in the Supplementary Information). Interestingly, among these potential hits, CREB2 is involved in the control of many metabolic processes, including glucose, lipid, and amino acid metabolism. (Yoshizawa et al., 2009; Wang et al., 2010; Ye et al., 2010). Moreover, a sequence in the human *SIRT4* promoter displayed significant homology with the canonical CREB recognition motif TGAYGYAA (Y = C or T) (Figure 3D). To determine whether CREB2 is involved in the mTORC1-dependent regulation of *SIRT4*, we performed RNAi experiments. The silencing of CREB2 abolished the rapamycin-induced expression of *SIRT4* (Figures 3E & S3A). Remarkably, the knockdown of CREB1 did not affect the upregulation of *SIRT4* upon mTORC1 inhibition, thus demonstrating the specificity of CREB2 to induce *SIRT4* (Figure S3B). Moreover, the knockdown of CREB2 significantly abrogated the rapamycin-induced increase in the activity of the *SIRT4* promoter, as determined by using a pGL3 luciferase reporter containing the putative CREB2 binding sequence (Figure 3F). Finally, chromatin immunoprecipitation (ChIP) assays revealed that CREB2 binds *SIRT4* during conditions of mTORC1 inhibition (Figure 3G).

mTORC1 regulates the stability of CREB2

We next investigated whether the mTORC1 pathway regulates CREB2. Although we did not observe major changes in *Creb2* mRNA in normal growth conditions (Figure S4A), mTORC1 inhibition resulted in accumulation of CREB2 protein levels by 2h of rapamycin treatment (Figure 4A). U0126 failed to cause the accumulation of CREB2 (Figure S4B). In contrast, CREB1 protein levels were not affected after 24h rapamycin treatment (Figure S4C). As observed for SIRT4, mTOR catalytic inhibitors, and the specific knockdown of mTOR, resulted in upregulation of CREB2 protein levels (Figures S4D & S4E). CREB2 is upregulated in diverse cell types as a response to a variety of stresses, including hypoxia, DNA damage, and withdrawal of GFs, glucose, and aa (Cherasse et al., 2007; Rouschop et al., 2010; Yamaguchi et al., 2008; Whitney et al., 2009). Interestingly, mTORC1 is negatively regulated by all of these environmental inputs (Zoncu et al., 2011). Since mTORC1 signaling in *Tsc2*−/− MEFs is insensitive to serum deprivation, we assessed the role of aa withdrawal and re-stimulation on CREB2 levels. As shown in Fig. 4B, CREB2 accumulated upon aa deprivation, and was decreased following aa re-addition. This phenomenon required the action of the proteasome as MG132 efficiently blocked CREB2 degradation following aa re-addition. Importantly, we found that mTORC1 inhibition abrogated the aa-induced decrease of CREB2 (Figure 4B). Similarly, MG132 protected CREB2 levels after insulin stimulation in *Tsc2*-WT MEFs (Figure S4F). These data suggest that mTORC1 regulates the stability of the CREB2 protein in our model. Consistent with this, cycloheximide (CHX) treatment revealed that the increase in CREB2 abundance following mTORC1 inhibition is due to increased CREB2 half-life (Figure 4C). Taken together, our data demonstrate that CREB2 accumulation following mTORC1 inhibition primarily occurs through a post-transcriptional mechanism.

NIH-PA Author Manuscript

NIH-PA Author Manuscript

NIH-PA Author Manuscript

mTORC1 activation promotes the binding of CREB2 to βTrCP and modulates CREB2 ubiquitination

Next, we attempted to identify the E3 ubiquitin ligase that might be responsible for CREB2 turnover. Consistent with a recent study, we found CREB2 to bind the E3 ligase, βTrCP (Frank et al., 2010). However, other related E3 ligases including Fbxw2, Fbxw7a, and Fbxw9 did not bind to CREB2 (data not shown). The interaction of CREB2 with Flag-βTrCP1 was enhanced in the presence of insulin, and was abolished by rapamycin pretreatment (Figure 4D). Importantly, insulin treatment promoted the ubiquitination of CREB2 in an mTORC1-dependent fashion (Figure 4E). Altogether, our results support the notion that the mTORC1 pathway regulates the targeting of CREB2 for proteasome-mediated degradation. βTrCP binds substrates via phosphorylated residues in conserved degradation motifs (degrons), typically including the consensus sequence DpSGX(n)pS or similar variants. We found an evolutionary conserved putative βTrCP binding site (**DSGXXXS**) in CREB2 (Figure 4F). Interestingly, we noted a downward mobility shift in CREB2 protein with mTORC1 inhibition, consistent with a possible decrease in the phosphorylation of CREB2. (Figure 4A). Frank et al. (2010) showed that phosphorylation of the first serine in the degron motif corresponding to Ser218 is required for the CREB2/βTrCP interaction, and this modification acts as a priming site for a gradient of phosphorylation events on five proline-directed residues codons (T212, S223, S230, S234, and S247) that is required for CREB2 degradation during the cell cycle progression (Frank et al., 2010). Consistent with these observations, we found that the mutation of the five residues to alanine (5A mutant) resulted in strong stabilization of CREB2, comparable to the serine-to-alanine mutation on the priming Ser218 phosphorylation site (Figure S4G). Single point mutations on each residue did not significantly increase stability compared with CREB2 WT (data not shown). Finally, to confirm the role of these five residues on the regulation of SIRT4, we expressed Flag-CREB2 WT, S218A, and 5A in serum starved HEK293E. As shown in Fig. 4G, insulin addition to cells expressing an empty vector (EV) resulted in decreased SIRT4 levels, a phenomenon abrogated by rapamycin pretreatment. SIRT4 levels were upregulated in cells expressing Flag-CREB2 WT, S218A and 5A when compared to control cells. However, only the expression of either S218A and 5A mutants was able to block the insulin-mediated decrease of SIRT4 (Figure 4G). Taken together, we demonstrate that the mTORC1 pathway promotes the destabilization of CREB2 to downregulate *SIRT4* expression.

SIRT4 represses bioenergetics and cell proliferation

We observed that glutamine utilization is repressed by rapamycin treatment (Figure 1) and SIRT4 is induced by mTORC1 inhibition (Figure 2). Thus, we tested whether SIRT4 itself directly regulates cellular glutamine uptake. The stable expression of SIRT4 resulted in the repression of glutamine uptake in *Tsc2*−/− MEFs and DLD1 cells (Figures 5A & 5B). Glucose uptake was not affected by SIRT4 expression (data not shown). Because glutamine can be an important nutrient for energy production, we examined ATP levels in SIRT4 expressing cells. Consistent with reduced glutamine consumption, the expression of SIRT4 in *Tsc2*−/− cells resulted in decreased ATP/ADP ratio compared to control cells (Figure 5C). Cells produce ATP via glycolysis and oxidative phosphorylation (OXPHOS). To test the contribution of mitochondrial metabolism versus glycolysis to ATP, we measured the ATP/ADP ratio after the treatment with oligomycin, an inhibitor of ATP synthesis from OXPHOS. Importantly, the difference of the ATP/ADP ratio between control and SIRT4 expressing cells was abrogated by oligomycin (Figure 5C), further demonstrating that SIRT4 may repress the ability of cells to generate energy from mitochondrial glutamine catabolism. Mitochondrial glutamine catabolism is essential for energy production and viability in the absence of glucose (Yang et al., 2009, Choo et al., 2010). Thus, we examined the effect of SIRT4 on the survival of *Tsc2*−/− MEFs during glucose deprivation. Control

NIH-PA Author Manuscript

NIH-PA Author Manuscript

NIH-PA Author Manuscript

cells remained viable following 48h of glucose deprivation. Conversely, SIRT4 expressing cells showed a dramatic increase in cell death under glucose-free conditions, which was rescued by the addition of the cell permeable dimethyl-ĮKG (DM-ĮKG) (Figure 5D). Conversely, the expression of SIRT4 did not affect the viability of glucose-deprived *Tsc2* WT MEFs (Figure S5A). Glucose deprivation also induced death of the human DU145 cancer cell line stably expressing SIRT4 (data not shown).

Glutamine is an essential metabolite for proliferating cells, and many cancer cells exhibit a high rate of glutamine consumption (DeBerardinis et al., 2007). Thus, decreased glutamine uptake in DLD1 and DU145 cancer cells expressing SIRT4 might result in decreased proliferation. Indeed, these cells grew significantly slower than did control cells. Remarkably, DM-ĮKG completely abrogated the decreased proliferation of SIRT4 expressing cells (Figure 5E & 5F), suggesting that repressed glutamine metabolism drove the reduced proliferation of cells expressing SIRT4. The expression of SIRT4 also slowed the proliferation of *Tsc2*−/− MEFs but did not affect *Tsc2* WT MEFs (Figures S5B & S5C). Finally, to rule out that the effect on proliferation was due to aberrant localization and to off-target effects of the overexpressed protein, we examined the localization of HA-SIRT4. We found that SIRT4 is co-localized with the MitoTracker, a mitochondrial-selective marker (Figure S5D). Taken together, these data demonstrate that SIRT4 is a critical negative regulator of mitochondrial glutamine metabolism and cell proliferation.

SIRT4 represses TSC-tumor development

Recent studies have demonstrated a major role of glutamine metabolism in driving oncogenic transformation of many cell lines (Gao et al., 2009; Wang et al., 2011). Since SIRT4 expression represses glutamine uptake and cell proliferation (Figure 5), we hypothesized that it could affect tumorigenesis. To test this idea, we assessed the role of SIRT4 in cell transformation by using an anchorage-independent growth assay. SIRT4 expression reduced the ability of *Tsc2*−/−*p53*−/− MEFs to grow in soft agar. However, the expression of SIRT4 in *Tsc2*+/+*p53*−/− did not impair their colony formation properties (Figure 6A). Next, we performed xenograft assays to investigate the impact of SIRT4 in cell growth *in vivo*. We inoculated *Tsc2*−/−*p53*−/− and *Tsc2*+/+*p53*−/− MEFs, stably expressing SIRT4 or vector control, subcutaneously, bilaterally, into nude mice (n=8 per group). Tumor incidence in mice injected with *Tsc2*+/+*p53*−/− MEFs was not affected by SIRT4 (data not shown). Conversely, in the *Tsc2*−/−*p53*−/− cohort, SIRT4 reduced tumor incidence by 20 days at median (Figure 6B). Furthermore, at post-inoculation day 80, mice injected with SIRT4 cells had a mean tumor volume of 246.1 ± 124.1 mm^3, whereas mice injected with control cells had mean tumor volume of 589.1 ± 101.5 mm^3 ($p<0.05$) (Figure 6C). As expected, SIRT4 and control tumors were immunoreactive for phospho-S6 (Figure 6D) and expressed HA-SIRT4 (Figure S6). Furthermore, SIRT4 expression in *Tsc2*−/−*p53*−/− MEFs resulted in reduction of Ki-67 positivity by 60% (Figure 6E), consistent with the finding that SIRT4 inhibits the proliferation of these cells *in vitro* (Figure S5B). Finally, we performed a comprehensive meta-analysis of *SIRT4* expression in human tumors and found significantly lower expression levels of *SIRT4*, relative to normal tissue, in bladder, breast, colon, gastric, ovarian and thyroid carcinomas (Figure 6F). Interestingly, loss of *SIRT4* expression showed a strong association with shorter time to metastasis in patients with breast cancer (Figures 6G & 6H). Altogether, these data strongly suggest that SIRT4 delays tumorigenesis regulated by the mTORC1 pathway.

The pharmacologic inhibition of glutamine anaplerosis synergizes with glycolytic inhibition to induce the specific death of mTORC1 hyperactive cells

The activation of mTORC1 leads to glucose and glutamine addiction as a result of increased uptake and metabolism of these nutrients (Choo et al., 2010; Duvel et al., 2010 & Figure 1).

NIH-PA Author Manuscript

NIH-PA Author Manuscript

NIH-PA Author Manuscript

These observations suggest that targeting this addiction offers an interesting therapeutic approach for mTORC1-driven tumors. The alkylating agent, mechlorethamine (Mechlo), incites cell toxicity in part by the inhibition of the GAPDH step of glycolysis via poly-ADP ribose polymerase (PARP)-dependent cellular consumption of cytoplasmic NAD^+. The ultimate consequence is glycolytic inhibition, thus mimicking glucose deprivation (Zong et al., 2004). Treatment of *Tsc2*−/− MEFs with Mechlo decreased both NAD levels and lactate production (Figure 7A and data not shown). The decrease in NAD^+ levels was rescued by addition of DPQ (Figure 7A), a PARP inhibitor (Zong et al., 2004). We next tested the ability of glutamine inhibition to determine the sensitivity of *Tsc2*−/− MEFs to Mechlo. As shown in Figure 7B, the treatment with EGCG, a GDH inhibitor (Figure 1G), potently synergized with Mechlo to kill *Tsc2*−/− MEFs with the greatest effect observed at 30μM (Figure 7B). As a result, this combination dramatically increased the cleavage of PARP, an apoptotic marker (Figure 7E). Similarly, glutamine deprivation sensitized *Tsc2*−/− MEFs to Mechlo (data not shown). The RNAi-mediated knockdown of GDH also synergized with Mechlo to induce death of *Tsc2*−/− MEFs (Figure 7D). Importantly, at these concentrations the combination did not induce death of a *Tsc2*-rescued cell line (Figure 7C).

Because the metabolic properties of cells with activated mTORC1 by *Tsc2*- deficiency can be efficiently targeted, we also examined other cell types in which mTORC1 is hyperactive by the loss of *PTEN*. We found that the combination of Mechlo and EGCG was also effective to induce specific toxicity of *PTEN*−/− MEFs, while *PTEN*+/+ MEFs were not affected (Figures S7A & S7B). In addition, the *PTEN*-deficient human prostate adenocarcinoma cell line, LNCaP, was also sensitive to treatment with Mechlo and EGCG (Figure 7F). This effect was specifically due to lack of TCA cycle replenishment as pyruvate supplementation completely reversed the synergistic effect (Figure 7F). The combination of Mechlo with the GLS1 inhibitor, BPTES (Figure 1G), also resulted in decreased viability of *Tsc*2−/− cells but not of Tsc2-reexpressing cells (Figures S7C & S7D). Again, death in *Tsc2*−/− cells was rescued with pyruvate or OAA (Figure S7E). To further investigate if the potent cell death in *Tsc2*−/− was restricted to Mechlo, we used 2-DG, a glycolytic inhibitor. The combination of 2-DG with either EGCG or BPTES resulted in enhanced cell death of *Tsc2*−/− MEFs compared to single agent treatments (Figure S7F). This effect was also specific to *Tsc2*−/− cells, since this combination was less toxic in Tsc2-reexpressing MEFs (Figure S7G). Taken together, our results demonstrate that the combination treatments aimed at inhibiting glycolysis and glutaminolysis potently synergize to kill cells with hyperactive mTORC1 signaling.

Discussion

Here, we define a novel mTORC1-regulated pathway that controls glutamine-dependent anaplerosis and energy metabolism (Figure 7G). We discovered that the mTORC1 pathway regulates glutamine metabolism by promoting the activity of GDH (Figures 1-3). We show that this regulation occurs by repressing the expression of *SIRT4*, an inhibitor of GDH (Figures 2 & 3). Molecularly, this is the result of mTORC1-dependent proteasome-mediated degradation of the *SIRT4* transcriptional regulator, CREB2 (Figure 4). Interestingly, the modulation of CREB2 levels correlates with increased sensitivity to glutamine deprivation (Ye et al., 2010; Qing et al., 2012), fitting with our model of glutamine addiction as a result of mTORC1 activation (Choo et al., 2010). Our data suggest that mTORC1 promotes the binding of the E3 ligase, βTrCP, to CREB2 (Figure 4D), promoting CREB2 degradation by the proteasome (Figure 4E). A previous study has demonstrated that five residues in CREB2 located next to the βTrCP degron are required for its stability (Frank et al., 2010). Accordingly, the mutation of these residues to alanine resulted in stabilization of CREB2 and SIRT4 following insulin and aa-dependent mTORC1 activation (Figure 4G). Future

NIH-PA Author Manuscript

NIH-PA Author Manuscript

NIH-PA Author Manuscript

work is aimed at determining if mTORC1 and/or downstream kinases are directly responsible for the multisite phosphorylation of CREB2.

The identification of CREB2 as an mTORC1-regulated transcription factor increases the repertoire of transcriptional regulators modulated by this pathway including HIF1α (glycolysis), Myc (glycolysis) and SREBP1 (lipid biosynthesis) (Duvel et al., 2010; Yecies and Manning, 2011). The oncogene Myc has also been linked to the regulation of glutamine metabolism by increasing the expression of the surface transporters ASCT2 and SN2, and the enzyme GLS. Thus, enhanced activity of Myc correlates with increased glutamine uptake and glutamate production (Wise et al., 2008; Gao et al., 2009). Our findings describe a new level of control to this metabolic node as shown by the modulation of the glutamate-to-αKG flux (Figure 2). This regulation is particularly relevant as some cancer cells produce more than 50% of their ATP by oxidizing glutamine-derived αKG in the mitochondria (Reitzer et al JBC, 1979). Therefore, these studies support the notion that Myc and CREB2/SIRT4 cooperate to regulate the metabolism of glutamine to αKG. Interestingly, Myc function may also be regulated by mTORC1 (West et al., 1998), although the mechanism is not known. Thus, besides controlling CREB2/SIRT4/GDH, mTORC1 might also influence the Myc/GLS axis, explaining the decrease of glutamine uptake observed in rapamycin-treated cells (Figure 1).

Our studies reveal the important impact of SIRT4 function on glutamine anaplerosis and tumor cell metabolism. Importantly, SIRT4 expression is decreased in a panel of human cancers, and we show that its expression results in decreased cell transformation and tumor development in a TSC-xenograft model (Figure 6). SIRT3 also represses tumorigenesis by regulating both genomic instability and the Warburg effect (Kim et al., 2010, Finley et al., 2011). Thus, these two mitochondrial sirtuins seem to function coordinately to modulate cell proliferation by controlling the two major nutrient sources required for tumor cell anabolism.

Glutamine is the main precursor for GSH synthesis despite sufficient glucose and oxygen levels, and the pharmacologic inhibition of GLS results in increased ROS and decreased proliferation (Le et al., 2012). Therefore, the importance of the glutamine pathway as a substrate for the TCA cycle, or as a regulator of redox homeostasis may be important for cancer cell adaption and survival. As a proof of concept, we show that inhibition of glutamine metabolism synergizes with glycolytic attenuation to induce robust death of *Tsc2*−/− cells, while their normal counterparts were not sensitive to dual inhibition. EGCG, an antioxidant found in green tea extracts and a potent inhibitor of GDH (Li et al., 2006) is already in several clinical trials as an anticancer agent and has been shown to be effective in limiting tumor growth in mice (Li et al., 2006; Khan and Mukhtar, 2008; Xu et al., 1992, Zhang et al., 2010).

Our findings shed new light on potential therapeutic strategies for cancers and genetic disorders characterized by deregulation of the mTORC1 pathway, such as TSC and LAM. Recently, rapamycin analogs showed efficacy in reducing the size of angiomyolipomas in clinical trials of TSC (Bissler et al., 2008). Moreover, these agents stabilized respiratory function and were associated with improvement in quality of life of LAM patients (McCormack et al., 2011). However, although the response to rapamycin was significant, effects were cytostatic, and tumor growth was observed after therapy cessation (Bissler et al., 2008), highlighting the need to develop specific agents for therapeutic intervention. TSC tumors display low Fluorodeoxyglucose (FDG) uptake in PET scanning (Young et al., 2009), suggesting that a source other than glucose fuels these tumors for survival; glutamine is likely to be such a source. Interestingly, we observed increased cell death of patient-derived LAM cells cultured under glutamine deprivation (data not shown). Therefore, we

NIH-PA Author Manuscript

NIH-PA Author Manuscript

NIH-PA Author Manuscript

speculate that targeted inhibition of glutaminolysis may induce tumor cell toxicity in LAM patients.

In sum, our work illustrates that mTORC1 inhibits the activity of GDH, by regulating the transcription of *SIRT4*. Moreover, our studies support the rationale of using PET imaging by 4-fluoroglutamine for mapping glutaminolytic tumors (Lieberman et al., 2011) and, importantly, the development of novel drugs targeting glutamine metabolism as cancer therapy.

Experimental Procedures

Cell lines and culture

Tsc2−/− *p53*−/− and *Tsc2*+/+ *p53*−/− MEFs were kindly provided by Drs. Brendan Manning and David Kwiatkowski (Harvard Medical School). ELT3 cells were provided by Dr. Cheryl Walker (University of Texas). All the other cell lines were obtained from ATCC. MEFs, ELT3, HEK293T, and HEK293E cells were cultured in DMEM. DLD1, LNCaPs and DU145 cells were cultured in RPMI media (Mediatech). DMEM or RPMI were supplemented with 10% FBS (Dialyzed for deprivation experiments –Gibco). All DMEM lacking glucose, aa, L-glutamine or combinations were made from formulations provided by Sigma. All extra energetic additives that are often added to some DMEM formulations such as sodium pyruvate and succinate were excluded.

Cell number measurements

Tsc2−/− MEFs were grown on 6-well plates and treated as indicated, trypsinized, and resuspended in PBS, pH 7.2 in a total of 10mL. Cell number was immediately analyzed on a Z2 Coulter Counter, and results were graphed in Coulter®AccuComp® Software, gating between 12μm and 30μm.

Cell viability

Cell viability was determined as previously described (Choo et al., 2010).

Statistics

Data were expressed as average ± standard error of the mean (SEM) of at least three independent experiments. An unpaired, 2-tail student *t*-test was used to determine differences between two groups. For the tumor incidence study, statistical analyses were performed using the Log-rank (Mantel-Cox).

Supplementary Material

Refer to Web version on PubMed Central for supplementary material.

Acknowledgments

We thank members of the Blenis' laboratory for critical discussions and technical assistance. We are grateful to Brendan Manning (HSPH), Takashi Tsukamoto (John Hopkins), Alexandra Grassian and Jonathan Coloff in Joan Brugge's lab (HMS). We thank the Nikon Imaging Center for advice and assistance with microscopy. AC is a LAM Foundation Postdoctoral Fellow. SMF is a German

Research Foundation Fellow (FE-1185). GP is a Pfizer Fellow of the Life Sciences Research Foundation. SMJ was supported in part by National Research Foundation of Korea Grant funded by the Korean Government. This work was funded by the National Heart, Lung, and Blood Institute Grant HL098216 to J.Y., and the NIH Grant GM51405 to JB.

NIH-PA Author Manuscript

NIH-PA Author Manuscript

NIH-PA Author Manuscript

References

Bissler JJ, McCormack FX, Young LR, Elwing JM, et al. Sirolimus for angiomyolipoma in tuberous sclerosis complex or lymphangioleiomyomatosis. N Engl J Med. 2008; 358(2):140–51. [PubMed: 18184959]

Cherasse Y, Maurin AC, Chaveroux C, Jousse C, Carraro V, Parry L, Deval C, Chambon C, Fafournoux P, Bruhat A. The p300/CBP-associated factor (PCAF) is a cofactor of ATF4 for amino acid-regulated transcription of CHOP. Nucleic Acids Res. 2007; 35(17):5954–65. [PubMed: 17726049]

Choo AY, Kim SG, Vander Heiden MG, et al. Glucose addiction of TSC-null cells is caused by failed mTORC1-dependent balance of metabolic demand with supply. Mol Cell. 2010; 38(4):487–99. [PubMed: 20513425]

DeBerardinis RJ, Mancuso A, Daikhin E, Nissim I, Yudkoff M, Wehrli S, Thompson CB. Beyond aerobic glycolysis: transformed cells can engage in glutamine metabolism that exceeds the requirement for protein and nucleotide synthesis. Proc Natl Acad Sci U S A. 2007; 104:19345–19350. [PubMed: 18032601]

DeBerardinis RJ, Lum JJ, Hatzivassiliou G, Thompson CB. The biology of cancer: metabolic reprogramming fuels cell growth and proliferation. Cell Metabolism. 2008; 7:11–20. [PubMed: 18177721]

Durán RV, Oppliger W, Robitaille AM, Heiserich L, Skendaj R, Gottlieb E, Hall MN. Glutaminolysis activates Rag-mTORC1 signaling. Mol Cell. 2012; 47(3):349–58. [PubMed: 22749528]

Duvel K, Yecies JL, Menon S, Raman P, Lipovsky AI, Souza AL, Triantafellow E, Ma Q, Gorski R, Cleaver S, et al. Activation of a metabolic gene regulatory network downstream of mTOR complex 1. Mol Cell. 2010; 39:171–183. [PubMed: 20670887]

Fendt SM, Buescher JM, Rudroff F, Picotti P, Zamboni N, Sauer U. Tradeoff between enzyme and metabolite efficiency maintains metabolic homeostasis upon perturbations in enzyme capacity. Mol Syst Biol. 2010; 6:356. [PubMed: 20393576]

Finley LW, Carracedo A, Lee J, Souza A, Egia A, Zhang J, Teruya-Feldstein J, Moreira PI, Cardoso SM, Clish CB, Pandolfi PP, Haigis MC. SIRT3 opposes reprogramming of cancer cell metabolism through HIF1Į destabilization. Cancer Cell. 2011; 19(3):416–28. [PubMed: 21397863]

Frank CL, Ge X, Xie Z, Zhou Y, Tsai LH. Control of activating transcription factor 4 (ATF4) persistence by multisite phosphorylation impacts cell cycle progression and neurogenesis. J Biol Chem. 2010; 285(43):33324–37. [PubMed: 20724472]

Haigis MC, Guarente LP. Mammalian sirtuins--emerging roles in physiology, aging, and calorie restriction. Genes Dev. 2006; 20:2913–2921. [PubMed: 17079682]

Gao P, Tchernyshyov I, Chang TC, et al. c-Myc suppression of miR-23a/b enhances mitochondrial glutaminase expression and glutamine metabolism. Nature. 2009; 458(7239):762–5. [PubMed: 19219026]

Gwinn DM, Shackelford DB, Egan DF, Mihaylova MM, Mery A, Vasquez DS, Turk BE, Shaw RJ. AMPK phosphorylation of raptor mediates a metabolic checkpoint. Mol. Cell. 2008; 30:214–226. [PubMed: 18439900]

Haigis MC, Mostoslavsky R, Haigis KM, Fahie K, Christodoulou DC, Murphy AJ, Valenzuela DM, Yancopoulos GD, Karow M, Blander G, Wolberger C, Prolla TA, Weindruch R, Alt FW, Guarente L. SIRT4 inhibits glutamate dehydrogenase and opposes the effects of calorie restriction in pancreatic beta cells. Cell. 2006; 126(5):941–54. [PubMed: 16959573]

Inoki K, Li Y, Zhu T, Wu J, Guan KL. TSC2 is phosphorylated and inhibited by Akt and suppresses mTOR signalling. Nat. Cell Biol. 2002; 4:648–657. [PubMed: 12172553]

Inoki K, Zhu T, Guan KL. TSC2 mediates cellular energy response to control cell growth and survival. Cell. 2003; 115(5):577–90. [PubMed: 14651849]

Khan N, Mukhtar H. Multitargeted therapy by green tea polyphenols. Cancer Lett. 2008; 269:269–80. [PubMed: 18501505]

Kim E, Goraksha-Hicks P, Li L, Neufeld TP, Guan KL. Regulation of TORC1 by Rag GTPases in nutrient response. Nat. Cell Biol. 2008; 10:935–945. [PubMed: 18604198]

NIH-PA Author Manuscript

NIH-PA Author Manuscript

NIH-PA Author Manuscript

Kim HS, Patel K, Muldoon-Jacobs K, Bisht KS, Aykin-Burns N, Pennington JD, van der Meer R, Nguyen P, Savage J, Owens KM, Vassilopoulos A, Ozden O, Park SH, Singh KK, Abdulkadir SA, Spitz DR, Deng CX, Gius D. SIRT3 is a mitochondria-localized tumor suppressor required for maintenance of mitochondrial integrity and metabolism during stress. Cancer Cell. 2010; 17(1): 41–52. [PubMed: 20129246]

Kim SG, Hoffman GR, Poulogiannis G, Buel GR, Jang YJ, Lee KW, Kim BY, Erikson RL, Cantley LC, Choo AY, Blenis J. Metabolic Stress Controls mTORC1 Lysosomal Localization and Dimerization by Regulating the TTT-RUVBL1/2 Complex. Mol Cell. 2013; 49(1):172–85. [PubMed: 23142078]

Le A, Lane AN, Hamaker M, Bose S, Gouw A, Barbi J, Tsukamoto T, Rojas CJ, Slusher BS, Zhang H, Zimmerman LJ, Liebler DC, Slebos RJ, Lorkiewicz PK, Higashi RM, Fan TW, Dang CV. Glucose-independent glutamine metabolism via TCA cycling for proliferation and survival in B cells. Cell Metab. 2012; 15(1):110–21. [PubMed: 22225880]

Li C, Allen A, Kwagh J, Doliba NM, Qin W, Najafi H, Collins HW, Matschinsky FM, Stanley CA, Smith TJ. Green tea polyphenols modulate insulin secretion by inhibiting glutamate dehydrogenase. J. Biol. Chem. 2006; 281:10214–21. [PubMed: 16476731]

Lieberman BP, Ploessl K, Wang L, Qu W, Zha Z, Wise DR, Chodosh LA, Belka G, Thompson CB, Kung HF. PET imaging of glutaminolysis in tumors by 18F-(2S,4R)4-fluoroglutamine. J Nucl Med. 2011; 52(12):1947–55. [PubMed: 22095958]

Manning BD, Tee AR, Logsdon MN, Blenis J, Cantley LC. Identification of the tuberous sclerosis complex-2 tumor suppressor gene product tuberin as a target of the phosphoinositide 3-kinase/akt pathway. Mol. Cell. 2002; 10:151–162. [PubMed: 12150915]

McCormack FX, Inoue Y, Moss J, Singer LG, Strange C, Nakata K, Barker AF, Chapman JT, Brantly ML, Stocks JM, Brown KK, et al. Efficacy and safety of sirolimus in lymphangioleiomyomatosis. N Engl J Med. 2011; 364(17):1595–606. [PubMed: 21410393]

Menon, Manning. Common corruption of the mTOR signaling network in human tumors. Oncogene. 2008; (Suppl 2):S43–51. [PubMed: 19956179]

Nicklin P, Bergman P, Zhang B, Triantafellow E, Wang H, Nyfeler B, Yang H, Hild M, Kung C, Wilson C, et al. Bidirectional transport of amino acids regulates mTOR and autophagy. Cell. 2009; 136:521–534. [PubMed: 19203585]

Possemato R, Marks KM, Shaul YD, Pacold ME, Kim D, Birsoy K, Sethumadhavan S, et al. Functional genomics reveal that the serine synthesis pathway is essential in breast cancer. Nature. 2011; 476(7360):346–50. [PubMed: 21760589]

Qing G, Li B, Vu A, Skuli N, Walton ZE, Liu X, Mayes PA, Wise DR, Thompson CB, Maris JM, Hogarty MD, Simon MC. ATF4 regulates MYC-mediated neuroblastoma cell death upon glutamine deprivation. Cancer Cell. 2012; 22(5):631–44. [PubMed: 23153536]

Reitzer LJ, Wice BM, Kennell D. Evidence that glutamine, not sugar, is the major energy source for cultured HeLa cells. J Biol Chem. 1979; 254(8):2669–76. [PubMed: 429309]

Rouschop KM, van den Beucken T, et al. The unfolded protein response protects human tumor cells during hypoxia through regulation of the autophagy genes MAP1LC3B and ATG5. J Clin Invest. 2010; 120(1):127–41. [PubMed: 20038797]

Roux PP, Ballif BA, Anjum R, Gygi SP, Blenis J. Tumor promoting phorbol esters and activated Ras inactivate the tuberous sclerosis tumor suppressor complex via p90 ribosomal S6 kinase. Proc. Natl. Acad. Sci. USA. 2004; 101:13489–13494. [PubMed: 15342917]

Sancak Y, Peterson TR, Shaul YD, Lindquist RA, Thoreen CC, Bar-Peled L, Sabatini DM. The Rag GTPases bind raptor and mediate amino acid signaling to mTORC1. Science. 2008; 320:1496–1501. [PubMed: 18497260]

Shanware NP, Mullen AR, DeBerardinis RJ, Abraham RT. Glutamine: pleiotropic roles in tumor growth and stress resistance. J Mol Med (Berl). 2011; 89(3):229–36. [PubMed: 21301794]

Vander Heiden MG, Cantley LC, Thompson CB. Understanding the Warburg effect: the metabolic requirements of cell proliferation. Science. 2009; 324(5930):1029–33. [PubMed: 19460998]

Wang C, Huang Z, Du Y, Cheng Y, Chen S, Guo F. ATF4 regulates lipid metabolism and thermogenesis. Cell Res. 2010; 20(2):174–84. [PubMed: 20066008]

NIH-PA Author Manuscript

NIH-PA Author Manuscript

NIH-PA Author Manuscript

Wang JB, Erickson JW, Fuji R, Ramachandran S, Gao P, Dinavahi R, Wilson KF, Ambrosio AL, Dias SM, Dang CV, Cerione RA. Targeting mitochondrial glutaminase activity inhibits oncogenic transformation. Cancer Cell. 2011; 18(3):207–19. [PubMed: 20832749]

West MJ, Stoneley M, Willis AE. Translational induction of the c-myc oncogene via activation of the FRAP/TOR signalling pathway. Oncogene. 1998; 17(6):769–80. [PubMed: 9715279]

Whitney ML, Jefferson LS, Kimball SR. ATF4 is necessary and sufficient for ER stress-induced upregulation of REDD1 expression. Biochem Biophys Res Commun. 2009; 379(2):451–5. [PubMed: 19114033]

Wise DR, DeBerardinis RJ, Mancuso A, Sayed N, Zhang XY, Pfeiffer HK, Nissim I, Daikhin E, Yudkoff M, McMahon SB, Thompson CB. Myc regulates a transcriptional program that stimulates mitochondrial glutaminolysis and leads to glutamine addiction. Proc Natl Acad Sci U S A. 2008; 105(48):18782–7. [PubMed: 19033189]

Wise DR, Thompson CB. Glutamine addiction: a new therapeutic target in cancer. Trends Biochem Sci. 2010; 35(8):427–33. [PubMed: 20570523]

Xu Y, Ho CT, Amin SG, Han C, Chung FL. Inhibition of tobacco-specific nitrosamine-induced tumorigenesis in A/J mice by green tea and its major polyphenol as antioxidants. Cancer Res. 1992; 52:3875–9. [PubMed: 1617663]

Yamaguchi S, Ishihara H, Yamada T, Tamura A, Usui M, Tominaga R, Munakata Y, Satake C, Katagiri H, Tashiro F, et al. ATF4-mediated induction of 4E-BP1 contributes to pancreatic beta cell survival under endoplasmic reticulum stress. Cell Metab. 2008; 7(3):269–76. [PubMed: 18316032]

Yang C, Sudderth J, Dang T, Bachoo RM, McDonald JG, DeBerardinis RJ. Glioblastoma cells require glutamate dehydrogenase to survive impairments of glucose metabolism or Akt signaling. Cancer Res. 2009; 69(20):7986–93. [PubMed: 19826036]

Ye J, Kumanova M, Hart LS, Sloane K, Zhang H, De Panis DN, Bobrovnikova-Marjon E, Diehl JA, Ron D, Koumenis C. The GCN2-ATF4 pathway is critical for tumour cell survival and proliferation in response to nutrient deprivation. EMBO J. 2010; 29(12):2082–96. [PubMed: 20473272]

Yecies, Manning. mTOR links oncogenic signaling to tumor cell metabolism. J Mol Med (Berl). 2011; 89(3):221–8. [PubMed: 21301797]

Yoshizawa T, Hinoi E, Jung DY, Kajimura D, Ferron M, Seo J, Graff JM, Kim JK, Karsenty G. The transcription factor ATF4 regulates glucose metabolism in mice through its expression in osteoblasts. J Clin Invest. 2009; 119(9):2807–17. [PubMed: 19726872]

Young LR, Franz DN, Nagarkatte P, Fletcher CD, Wikenheiser-Brokamp KA, Galsky MD, Corbridge TC, Lam AP, Gelfand MJ, McCormack FX. Utility of [18F]2-fluoro-2-deoxyglucose-PET in sporadic and tuberous sclerosis-associated lymphangioleiomyomatosis. Chest. 2009; 136(3):926–33. [PubMed: 19349386]

Zhang D, Al-Hendy M, Richard-Davis G, Montgomery-Rice V, Sharan C, Rajaratnam V, Khurana A, Al-Hendy A. Green tea extract inhibits proliferation of uterine leiomyoma cells in vitro and in nude mice. Am J Obstet Gynecol. 2010; 202(3):289.e1–9. [PubMed: 20074693]

Zoncu R, Efeyan A, Sabatini DM. mTOR: from growth signal integration to cancer, diabetes and ageing. Nat Rev Mol Cell Biol. 2011; 12:21–35. [PubMed: 21157483]

Zong WX, Ditsworth D, Bauer DE, Wang ZQ, Thompson CB. Alkylating DNA damage stimulates a regulated form of necrotic cell death. Genes Dev. 2004; 18:1272–82. [PubMed: 15145826]

NIH-PA Author Manuscript

NIH-PA Author Manuscript

NIH-PA Author Manuscript

Highlights

1. mTORC1 regulates glutamine anaplerosis.
2. mTORC1 represses the transcription of *SIRT4* to regulate GDH activity.
3. SIRT4 represses cell proliferation and is downregulated in human cancer.
4. Glutamine and glucose metabolism inhibition results in death of cancer cells.

NIH-PA Author Manuscript
NIH-PA Author Manuscript
NIH-PA Author Manuscript

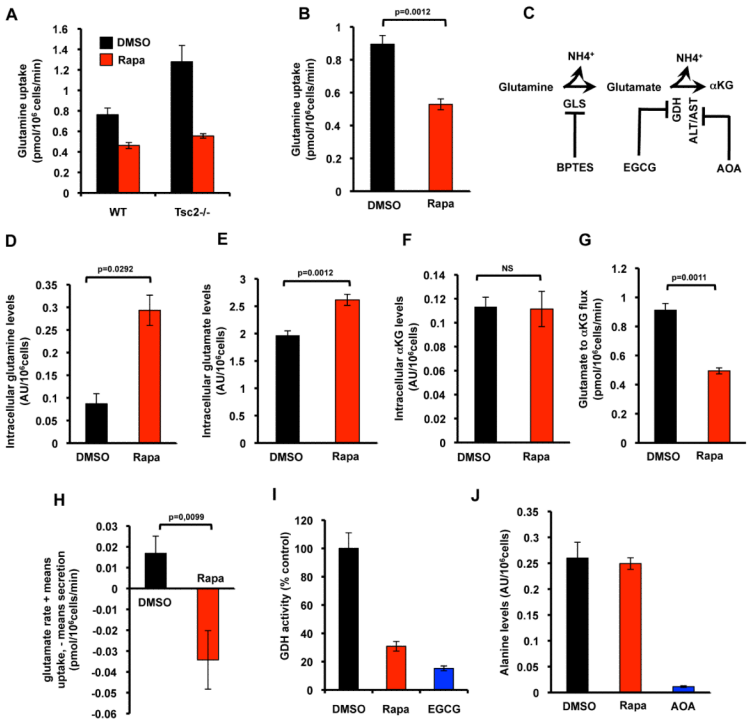

Figure 1. The mTORC1 pathway regulates glutamine metabolism via glutamate dehydrogenase

Glutamine uptake was determined in: **(A)** *Tsc2*-WT and *Tsc2*−/− MEFs treated with rapamycin; and **(B)** DLD1 cells treated with rapamycin. **(C)** A diagram showing the enzymes involved in glutamine anaplerosis and the inhibitors used in this study (See text for more details). Intracellular levels of glutamine **(D)**, glutamate **(E)**, and αKG **(F)** in DLD1 cells treated with rapamycin. **(G)** Glutamate-to-αKG flux was determined in DLD1 cells treated with rapamycin. **(H)** Glutamate secretion rates in DLD1 cells treated as in (B). **(I)** GDH activity in DLD1 cells treated with rapamycin. EGCG was used as a positive control. **(J)** Alanine levels were determined in DLD1 cells treated with rapamycin or AOA. AU: arbitrary units. The mean is shown; error bars represent SEM (n>3). See also Figure S1.

NIH-PA Author Manuscript

NIH-PA Author Manuscript

NIH-PA Author Manuscript

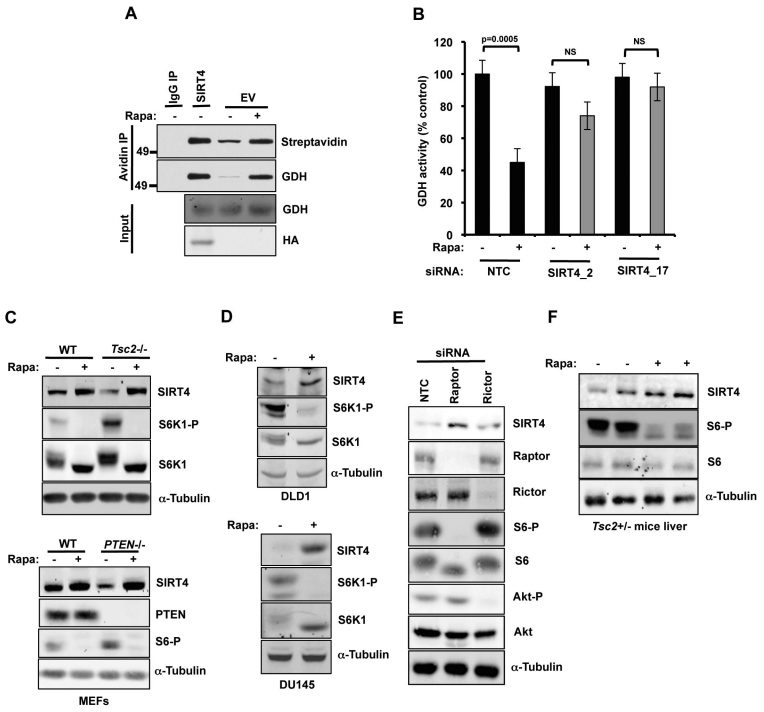

Figure 2. mTORC1 controls glutamate dehydrogenase activity by repressing SIRT4

(A) DLD1 cells treated with rapamycin followed by analysis of mono-ADP-ribosylated GDH as described in the experimental procedures. DLD1 cells stably expressing SIRT4-HA were used as a positive control. **(B)** GDH activity was determined in *Tsc2*−/− MEFs transfected with a non-targeting control siRNA (NTC) or two independent siRNAs against SIRT4, and then treated with rapamycin for 24h. SIRT4 protein levels in whole cell lysates from: **(C)** *Tsc2*-WT, *Tsc2*−/− MEFs; and *PTEN*-WT, *PTEN*−/− MEFs treated as in (A); **(D)** DLD1 and DU145 cells treated as in (A); **(E)** *Tsc2*−/− MEFs transfected with a non-targeting control (NTC) siRNA or siRNAs targeting either raptor or rictor; and **(F)** The liver of *Tsc2*+/− mice treated with rapamycin. The mean is shown; error bars represent SEM (n>3). See also Figure S2.

NIH-PA Author Manuscript

NIH-PA Author Manuscript

NIH-PA Author Manuscript

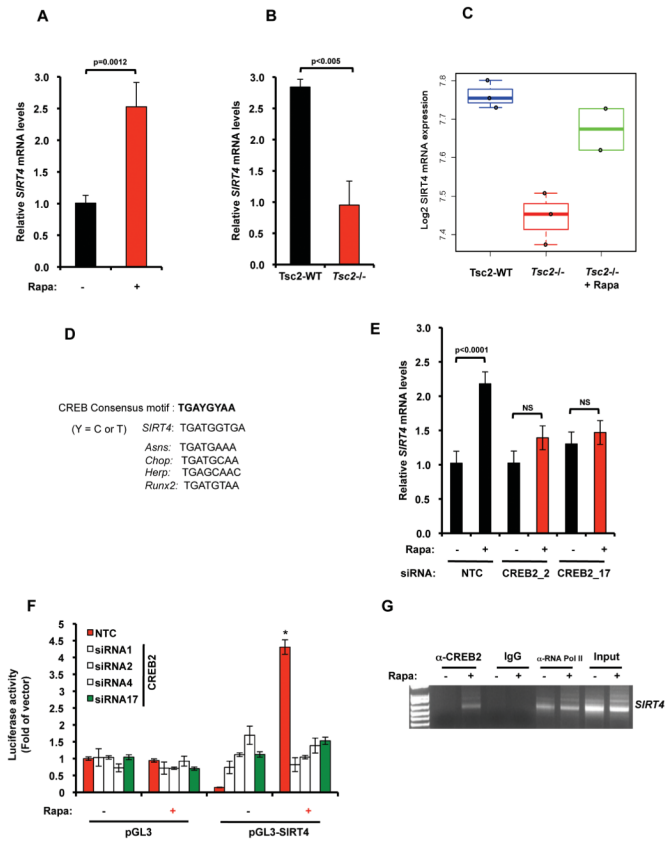

Figure 3. SIRT4 is regulated at the mRNA level in an mTORC1-dependent fashion

(A) *SIRT4* mRNA levels in *Tsc2*−/− MEFs treated with rapamycin for 24h. **(B)** *SIRT4* mRNA levels in *Tsc2*−/− and *Tsc2*-WT MEFs as in (A). **(C)** Box-plots of *SIRT4* expression in Tsc2-WT (blue) and *Tsc2*−/− MEFs without (red) or with (green) rapamycin treatment **(D)** CREB-binding consensus motif identified on several CREB target gene promoters and the human *SIRT4* gene promoter. The putative CREB recognition sequence on the human *SIRT4* promoter was aligned with other established CREB recognition sequences. **(E)** *SIRT4* mRNA levels in *Tsc2*−/− MEFs transfected with non-targeting siRNA (NTC) or with two independent siRNAs against CREB2. Cells were treated with rapamycin for 24h. **(F)** Normalized luciferase light units of CREB2 knocked-down *Tsc2*−/− transfected with a pGL3-luciferase reporter construct or with pGL3-SIRT4. Twenty-four hours after transfection cells were treated with DMSO or rapamycin for 24h (*p<0.05). **(G)** *Tsc2*−/− MEFs were incubated in the presence or absence of rapamycin and were then harvested for ChIP analysis using an anti-CREB2 antibody or pre-immune IgG. Specific primers were used to amplify *SIRT4*. Input chromatin was diluted to 1:1000. α-RNA Pol II was used as a positive control. All PCR products were resolved by 2% agarose electrophoresis. The mean is shown; error bars represent SEM (n>3). See also Figure S3

NIH-PA Author Manuscript

NIH-PA Author Manuscript

NIH-PA Author Manuscript

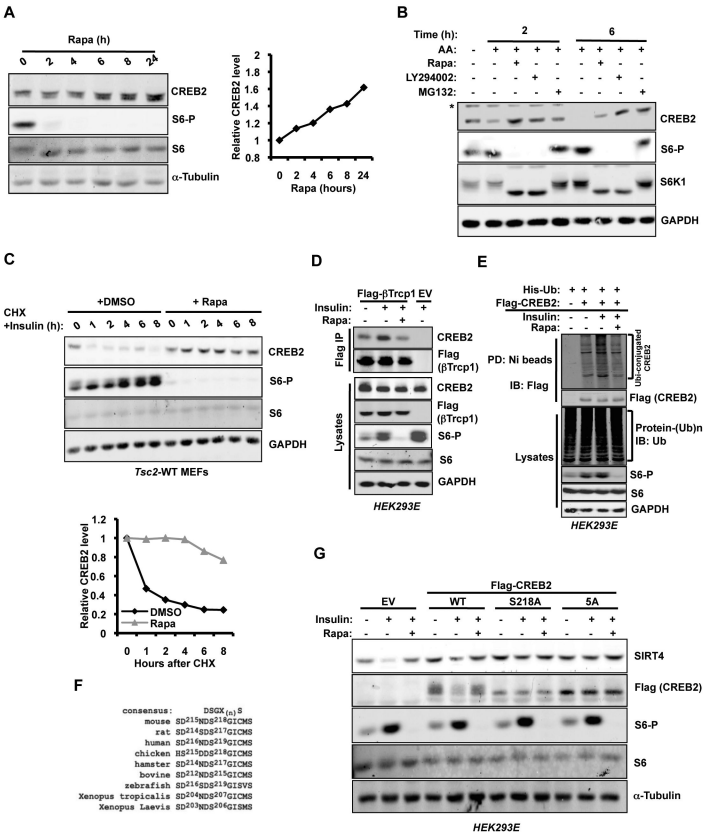

Figure 4. mTORC1 regulates the stability of CREB2

(A) Immunoblot analysis of CREB2 in *Tsc2*−/− MEFs treated with rapamycin. Cells were harvested at the indicated time points. The right panel shows the quantification of band intensities. CREB2 bands were normalized to α-Tubulin, then normalized to the *t*=0 time point. **(B)** *Tsc2*−/− MEFs were amino acid (AA) and serum starved for 18h and pre-treated with the indicated drugs for 30 min, followed by addition of AA for 2 or 6h. Protein lysates were resolved by immunoblot using the antibodies indicated. The asterisk (*) denotes a nonspecific band. **(C)** *Tsc2*-WT MEFs were serum starved for 18h and were pre-treated with rapamycin or DMSO for 30 min. 100nM insulin with 20μg/mL cycloheximide (CHX) was added to cells before harvesting. The bottom panel shows the quantification of band intensities. CREB2 bands were normalized to GAPDH, then normalized to the *t* =0 time point. **(D)** HEK293E cells were transfected with constructs coding Flag-βTrCP1. 24h after transfection, cells were serum starved for 18h and pre-treated with rapamycin for 30min. 100nM insulin was then added to cells for 2h. Total protein lysates were subjected to immunoprecipitation using anti-Flag M2 antibody. **(E)** Flag-CREB2 was expressed in HEK293E cells together with His-Ub. Cells were serum starved for 18h and treated with MG132 for 4h. Then, cells were pre-treated with either DMSO or rapamycin for 30 min. 100nM insulin was added for 6h. His-ubiquitinated proteins were pulled-down with Ni-NTA agarose and analyzed by immunoblotting. **(F)** Schematic of the conserved βTrCP degrons in CREB2 across multiple species. **(G)** CREB2 mutants were expressed in HEK293E cells. These cells were serum starved for 18h and pre-treated with rapamycin for 30min. 100nM insulin was added to the media for 8h. See also Figure S4.

NIH-PA Author Manuscript
NIH-PA Author Manuscript
NIH-PA Author Manuscript

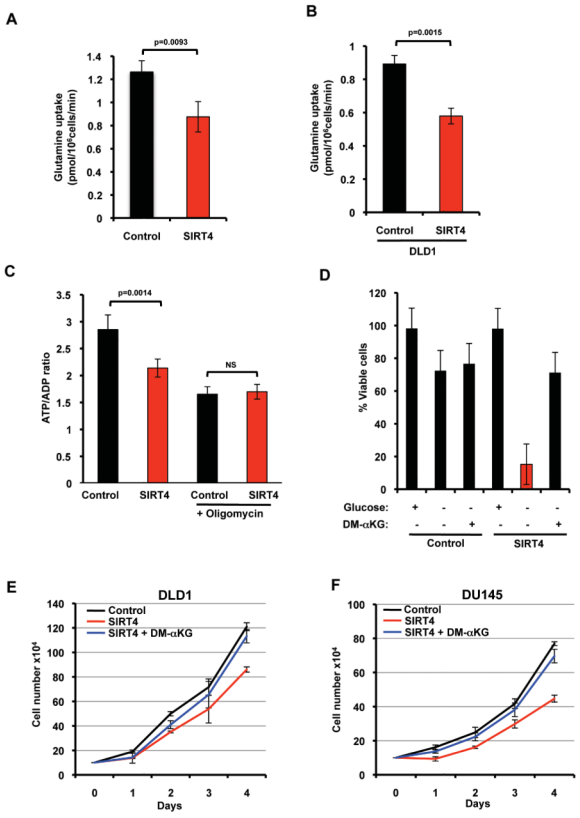

Figure 5. SIRT4 represses bioenergetics and proliferation

Glutamine uptake was determined in: **(A)** *Tsc2*−/− MEFs stably expressing SIRT4 or vector control; **(B)** DLD1 cells expressing SIRT4 or vector control. **(C)** The ATP/ADP ratio was measured in *Tsc2*−/− -control or SIRT4-expressing MEFs treated with or without oligomycin (5μg/mL). **(D)** Cell viability of control or SIRT4 expressing *Tsc2*−/− MEFs deprived of glucose and supplemented with DM-ĮKG (7mM) or pyruvate (1mM) for 48h. Growth curves of: DLD1 **(E)** and DU145 **(F)** cells stably expressing SIRT4 or vector control. Cells were cultured in standard media lacking pyruvate, and DM-αKG was added to media as indicated. Cell number was measured every 24h for four consecutive days. The mean is shown; error bars represent SEM (n>3). See also Figure S5.

NIH-PA Author Manuscript
NIH-PA Author Manuscript
NIH-PA Author Manuscript

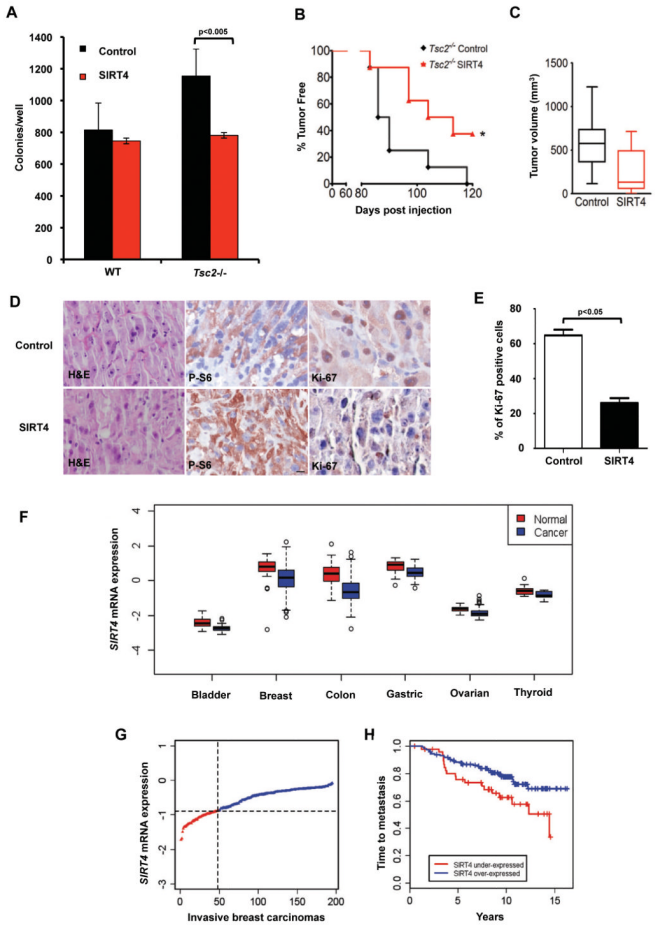

Figure 6. SIRT4 suppresses TSC-tumor development

(A) Soft agar assays using *Tsc2*−/− or *Tsc2*-WT MEFs expressing control vector or SIRT4. **(B)** Kaplan-Meier plot of the percentage of tumor-free mice after inoculation with *Tsc2*−/−*p53*−/− MEFs expressing control or SIRT4 vectors (n=8). *p<0.05. **(C)** Tumor volume and weight were measured. **(D)** Immunohistochemical analysis of Ki-67 and representative H&E staining (Original magnification, 20x). **(E)** Quantification of Ki-67 staining in tumors from (D). **(F)** Box-plots indicating significantly lower expression of *SIRT4* gene in bladder, breast, colon, gastric, ovarian and thyroid carcinomas compared to corresponding normal (*p<0.05). **(G)** Ranked *SIRT4* expression in a breast carcinoma dataset of 195 tumors. **(H)** Kaplan-Meier curve comparing time to metastasis between breast carcinomas with the lowest (<25th percentile) vs. highest (>25th percentile) *SIRT4* expression (p=0.02, log-rank test). The mean is shown; error bars represent SEM (n>3). See also Figure S6.

NIH-PA Author Manuscript
NIH-PA Author Manuscript
NIH-PA Author Manuscript

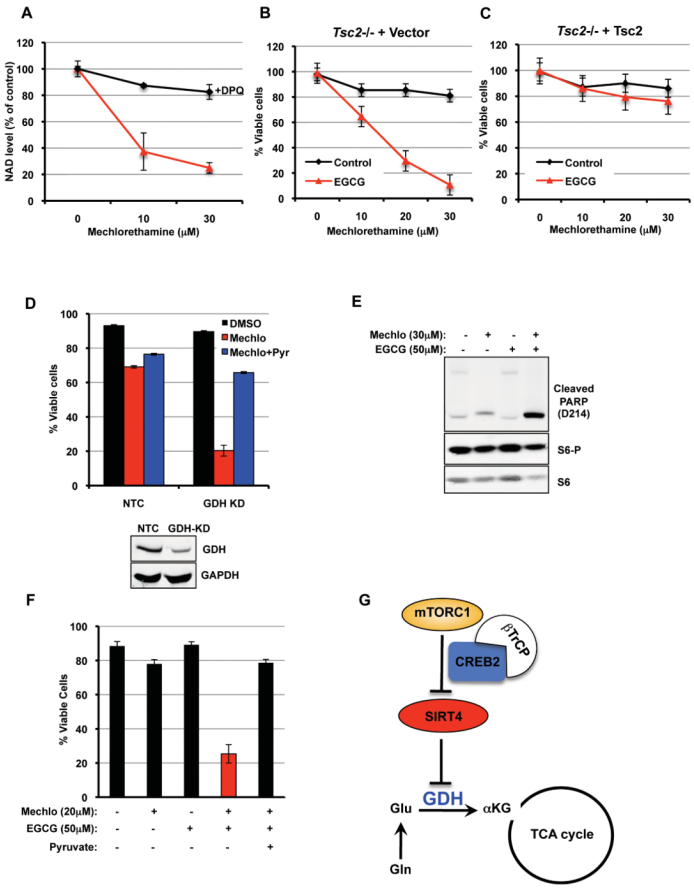

Figure 7. The combination of glutamine metabolism inhibitors with glycolytic inhibition is an effective therapy to kill Tsc2−/− and PTEN−/− cells

(A) NAD levels in *Tsc2*−/− MEFs treated with the indicated doses of Mechlorethamine with or without DPQ for 24h. **(B)** *Tsc2*−/− MEFs transduced with an empty vector were given the indicated doses of Mechlorethamine with or without EGCG (50μM). Cell viability was measured 48 hours post treatment via PI-exclusion. **(C)** *Tsc2*−/− MEFs re-expressing Tsc2 were treated as in (B). **(D)** *Tsc2*−/− MEFs were transfected with a non-targeting control siRNA (NTC) or siRNA targeting GDH. Twenty-four hours post-transfection cells were treated with 20μM of Mechlorethamine and cell viability was determined 48h later post treatment. **(E)** Immunoblot analysis of cleaved PARP in *Tsc2*−/− MEFs treated with Mechlorethamine (30μM) or EGCG (50μM), or the combination of both drugs for 24h. **(F)** Cell viability of LNCaP cells treated with Mechlorethamine or EGCG, or the combination of both drugs. Pyruvate was added to the media as indicated. **(G)** Schematic of the regulation of SIRT4 and glutamine metabolism by the mTORC1 pathway. The mean is shown; error bars represent SEM (n>3). See also Figure S7.